Transport and cooling of singly-charged noble gas ion beams

G. Ban, [a] G. Darius, [a] D. Durand, [a] X. Fléchard, [a] M. Herbane, [a] M. Labalme, [a] E. Liénard, [a] F. Mauger, [a] O. Naviliat-Cuncic, [a] C. Guenault, [b] C. Bachelet, [b] P. Delahaye, [c] A. Kellerbauer, [c] L. Maunoury, [d] J.Y. Pacquet [d]

[a] *Laboratoire de Physique Corpusculaire, Caen, France*
[b] *CSNSM, Orsay, France*
[c] *CERN-ISOLDE, Geneva, Switzerland*
[d] *LIMBE-GANIL, Caen, France*

Abstract

The transport and cooling of noble gas singly-charged ion beams by means of a Radio Frequency Quadrupole Cooler Buncher (RFQCB) have been studied at the LIMBE low energy beam line of the GANIL facility. Ions as light as $^4He^+$ have been cooled and stored before their extraction in bunches using H_2 as buffer gas. Bunches characteristics have been studied as a function of the parameters of the device. Sizeable transmissions of up to 10 % have been obtained. A detailed study of the lifetime of ions inside the buncher has been performed giving an estimate of the charge exchange cross-section. Results of a microscopic Monte-Carlo transport code show reasonable agreement with experimental data.

Key words: cooling, singly-charged ion beams, quadrupole radio frequency
PACS:

1 Introduction

Beam handling is nowadays a very active field of research in nuclear physics. In this context, Radio Frequency Quadrupole Cooler-Buncher (RFQCB) devices have shown to play an increasing role to manipulate radioactive beams near low energy facilities [1,2,3,4,5,6,7]. The Laboratoire de Physique Corpusculaire (LPC) in Caen has developped a RFQCB to cool and guide exotic ions produced near the SPIRAL facility at GANIL [8]. One of the planned experiments will focus on the precise measurement of the $\beta - \nu$ angular correlation

parameter in the β decay of ^6He [9]. Such a measurement allows to search for the possible existence of exotic couplings not allowed by the Standard Model [10]. The experiment will be performed inside a transparent Paul trap [11]. Unstable $^6He^+$ ions will be confined under high vacuum in a few mm^3 volume in the center of the trap. Following their β decay, coincidences between the β and the recoil ion, ^6Li, will be recorded. The radioactive ions will be provided by the LIRAT [12,13] beam line, a low energy radioactive isotope beamline at GANIL. It uses an Electron Cyclotron Resonance Ion Source for ion production after fragmentation reactions [14]. Because of the large temperature and electron density inside an ECR plasma, the ions are heated, and their temperature is in the few eV range inducing large emittances, up to 100 $\pi mm.mrad$ for ion kinetic energies near 30 keV. The use of a RFQCB filled with a buffer gas is thus intended to prepare the beam before injection inside the Paul trap in order to allow the trapping by reducing the initial emittance. The principle is to confine radially the ions by means of a radio frequency quadrupole field and to slow down their motion by collisions with the atoms or molecules of the so-called buffer gas. An additional electrostatic longitudinal field drives the ions towards the end of the device where they can be stored in a potential well and extracted as a bunch. They can then be efficiently injected in the Paul trap. We have performed an experiment using stable singly-charged ions produced by the LIMBE low energy beam line at GANIL [15]. After a description of the apparatus, the results concerning the cooling and bunching of $^4He^+$ and $^{40}Ar^+$ ions using He and H_2 as buffer gases are presented. They are compared with the outcome of a microscopic transport model.

2 The experiment

2.1 Experimental set-up

The experimental set-up is displayed in Fig.1. Ion beams come from the left and enter the system passing through a first Faraday Cup, FC1, used for monitoring purposes. Note also the presence of a thermo-ionic source perpendicular to the beam axis which can be used to produce alkaline ions. Data obtained for such ion beams will be discussed elsewhere [17]. Ions are then transported and focussed at the entrance of the RFQCB. This latter is placed on a high voltage platform whose voltage is 100 V lower than the extraction voltage of the ECR source. Therefore, incoming ions have kinetic energies close to 100 eV with respect to the RFQCB. Typical energies of singly-charged ions delivered by the LIMBE facility are a few keV [15]. The RFQCB is described in details elsewhere [18]. Since the mass of the constituents of the buffer gas must be lighter than the one of the ions, two light gases have been used: H_2 and the most commonly used He. The reason why H_2 had to be used in these

tests for $^4He^+$ ions is due to the strong charge exchange resonant process between He atoms and singly-charged He^+ ions. This is also the reason why the future experiment involving ^6He ions will use H_2. Ions are stored at the end of the RFQCB inside the buncher. After a variable time (hereafter called the "cooling" time, t_{cool}), ions are ejected by switching the configuration of the electrostatic potential as shown in Fig. 2. After extraction and passage thbrough a pulse-down electrode, the ion kinetic energy is close to 1 keV. The rest of the line is dedicated to the transport and the diagnostics (FC2) of the cooled beam up to the detection device consisting of a micro-channel plate (MCP).

2.2 Operating modes

Measurements have been carried out to observe the cooling and bunching of ions inside the RFQCB while varying the parameters of the device. Measurements were firstly performed with a continuous beam. Faraday cups were then used to measure beam currents at the entrance (FC1) and at the exit (FC2) of the RFQCB thus allowing to estimate the transmission through the device. However, in order to have access to the time dependence of the whole process, the ion beam delivered by LIMBE could be pulsed by applying a bias between two parallel plates located along the beam line with an adjustable duration between 1 and 5 ms, and a frequency between 10 and 100 Hz. Therefore, ions were swept away from the beam line when the bias was on and were transported towards the entrance of the RFQCB when the bias was off. Let t_0, be the instant when the beam passes through the plates. Since the time of flight between the deflecting plates and the entrance of the RFQCB is a constant for a given ion, t_0 can be safely used as a reference "start" for the study of the time dependance of the cooling and bunching process. The "cooling" time, t_{cool}, could be varied between 0 and 50 ms after t_0. Short values of t_{cool} (less than a ms) allow the study of the diffusion and transport of the incoming ions through the cooler-buncher as discussed in section 3.5 while larger values give access to the lifetime of the ions inside the buncher (see section 3.6).

2.3 Brief description of the transport model used for the simulations

A simulation tool has been developped to design the characteristics of the device and to compare with experimental data. It is described in details elsewhere [9,19]. This is a Monte Carlo code describing at the microscopic level the collisions between the incoming ions and the buffer gas. The kinematics and the rate of the collisions are estimated using interaction potentials as realistic as possible. These latter are "tested" by comparison of the results of the code

with experimental mobilities and diffusivities [20,21,22,23]. The transport of the ions in the electromagnetic environment is considered so that the total transmission process of the ions inside the cooler-buncher can be simulated including the storage inside the buncher.

3 Measurements

Since it was not possible to obtain either absolute calibrations of the FC's or the absolute efficiency of the MCP with sufficient accuracy, we have decided to normalize the experimental data to the results of the simulation. However, the transmissions obtained by measuring currents on the Faraday cups or by counting the ions on the MCP are comparable (within a factor 2) with the transmissions predicted by the Monte Carlo code.

3.1 Transmission: influence of the buffer gas pressure

We first address the evolution of the transmission through the RFQCB as a function of the buffer gas pressure. Fig. 3 and 4 show experimental results (black squares) measured in the continuous mode and the results of the calculation (lines) for resp. $^4He^+$ in H_2 and $^{40}Ar^+$ in He. Both distributions exhibit a maximum around 4-5 $mTorr$ for $^4He^+ + H_2$ and 5-6 $mTorr$ for $^{40}Ar^+ + He$. The transmission is low at low pressure because there are not enough collisions between ions and the buffer gas to properly guide the ions towards the exit of the buncher. As the pressure increases, the collision rate increases and hence the transmission. However, for large values of the pressure, the transmission decreases because there are then too many collisions so that ions are lost in the structure near the exit of the device. In other words, the size of the ion cloud is larger than the exit diameter of the apparatus. As far as calculations are concerned, although the maximum value is correctly reproduced, the distribution is much too narrow as compared to experimental data. A possible explanation lies in the fact that a constant homogeneous pressure has been assumed inside the RFQCB for the simulations. In principle, one should take into account a possible gradient of the pressure near the exit (and also the entrance) of the apparatus due to gas flow. This has not yet been implemented in the simulation.

3.2 Transmission: influence of the RF parameters

An exploration of the stability region has been undertaken by varying the Mathieu parameter, q, defined by:

$$q = \frac{4eV_0}{mr_0^2\omega^2} \tag{1}$$

where e is the charge of the ion, V_0 the potential applied to the rods of the quadrupole, m the ion mass, ω the radio-frequency and r_0 the radius of the quadrupole. In the case of $^4He^+ + H_2$, typical values are V_0=100 V and $\nu = \omega/2\pi$ between 1 and 2 MHz. As shown in Fig. 5, the maximum transmission is obtained (whatever the considered frequency) around q=0.5. This is in rough agreement with the calculation although this latter predicts a much larger range of optimal transmission starting around q=0.3-0.4: a fact that is not observed in the experimental data. A possible explanation lies on the distorsion of the RF outputs (which were not fully sinusoidal) for low values of the applied bias, V_0, corresponding to low values of q.

3.3 Optimized transmissions

In the continuous beam mode, transmissions have been estimated by comparing currents measured on the different FC's. There are uncertainties concerning these figures because the first FC (FC1) could not be placed close enough to the entrance of the RFQCB so that the flux measured by FC1 may be overestimated with respect to the actual flux entering the apparatus. More, as already mentionned, the FC's have not been calibrated on absolute values. We therefore estimate the uncertainty in the transmission measurement around a factor 2. A compilation is shown in Table 1. For all systems, a systematic exploration of the influence of the pressure and of the RF parameters has been performed and the numbers quoted in Table 1 correspond to optimal values. One should however note that for technical reasons, the q parameter could not be set to its optimum value (around 0.5) for all studied systems. Note also that the transmission for $^{40}Ar^+ + H_2$ is zero because of a strong charge exchange resonant effect due to the similarity of the values of the ionization potentials of these two species: 15.755 and 15.427 eV respectively. Apart from that, transmissions between 5 and 10 % have been obtained. No significant differences were observed for $^{22}Ne^+ + He$ and $^{22}Ne^+ + H_2$. As stated above, the measured transmissions are within the expectations of the simulation.

3.4 Time-of-flight measurement

We now consider the time-of-flight (ToF) distributions of the extracted bunches. This is achieved by measuring the time of arrival of the ions on the MCP detector with respect to the time associated with the switch in the potential configuration of the buncher as shown in Fig. 2. We first discuss the $^{40}Ar^{+}+He$ case in Fig. 6 and 7. In Fig. 6, the evolution of the mean value of the time-of-flight is shown as a function of the pressure for experimental data (black squares) and for simulated data (solid line). As expected, an increase of the ToF is observed as pressure increases. This is understood as the growth of collision rate near the exit of the buncher. In conjunction, the pressure has also an influence on the ToF width. Most of the time distribution width is due to the finite extent of the confined cloud of ions inside the buncher. Indeed, the electrostatic potential has such a structure (see Fig. 2) that ions are located in a region of the order of a few mm. When the electrostatic barrier is lowered down, those ions which are located close to the exit have a shorter travel inside the buncher and suffer less residual collisions with the gas than those located more inside the buncher. Hence, they have a shorter diffusion time towards the exit and this leads to a spread both in time and space of the bunches. These effects are correctly accounted for by the simulation although the model somehow underestimates the time width. The agreement is not so good when considering the $^{4}He^{+}+H_2$ case (Fig. 8 and 9). In particular, the width is there strongly overestimated by the simulation. One should note that the interaction potential for such a system is poorly known. In particular, for this system, it was not possible to confront the results of the model with experimental mobilities and/or diffusivities since these latter are not available. Therefore, the parameters of the potential were taken to be those of $^{6}Li^{+}$.

3.5 Measurement of the "cooling" time: t_{cool}

In order to understand in more details the transport properties ot the device, we have performed measurements of the time dependance of the transmission factor. To this end, the beam was pulsed as described previously in section 2.2. A short pulse was injected in the RFQCB and the extracted ions were detected and counted as a function of t_{cool}. For short values, this is a measure of the time needed for the ions to travel through the device before reaching the buncher. This quantity is mainly governed by the diffusion process of the ions throughout the gas and is therefore an interesting test as far as the validity of the simulations is concerned. Figs 10 and 11 show the results of the comparisons. For very short values of t_{cool}, ions have no time to reach the end of the device and there is no signal. As soon as typical values are applied of the order of a few hundreds μs, the transmission rapidly increases

and then saturates. Here, those ions which have survived their travel across the apparatus have all reached the buncher. A comparison of the results of the simulation with the data shows a rather good agreement although for the $^{40}Ar^{+}+He$ system, the saturation value of t_{cool} is slightly overestimated. It is worth noting that in order to obtain an experimental "clean" signal, it was found necessary to empty the cooler before each injection by extracting those ions from the previous injection which remained in the device.

3.6 Lifetimes

Extending the time measurement described in the previous section well above the ms regime allows to address the question of the lifetime of the ions stored inside the buncher. Measurements of the transmission have been performed up to 90 ms as shown in Fig. 12. For each pressure, an exponential fall-off in the time distribution has been observed and measured. A compilation of the results obtained for different combinations of ion-buffer gas is displayed in Fig. 13. The discussion of alkaline ions will be performed elsewhere: they are here only for a matter of comparison. The lifetime τ reads:

$$\tau = \frac{1}{\rho < \sigma_{CT} v_{rel} >} \tag{2}$$

where ρ is the buffer gas density and $< \sigma_{CT} v_{rel} >$ is the average product of the charge transfer cross-section and of the relative velocity between the ions and the buffer gas atoms or molecules. One then obtains:

$$\frac{1}{\tau} \propto p < \sigma_{CT} v_{rel} > \tag{3}$$

The inverse of the lifetime is proportionnal to the buffer gas pressure if the loss of ions is only due to charge exchange reactions. Using Eq. 3, we have access to the product $< \sigma_{CT} v_{rel} >$. In the case of $^{4}He^{+}+H_2$, one obtains experimentally: $\tau p \simeq 200\ ms.mTorr$ which leads to $< \sigma_{CT} v_{rel} > \simeq 1.4\ 10^{-13} cm^3/s$. This value is in good agreement with the value quoted in [24]. However, one should notice in Fig. 13 that the experimental values of the inverse of the lifetime do not cross the origin when the pressure is zero. We believe that the deviations observed are essentially due to uncertainties in the absolute values of the pressure and also probably to the presence of polluants such as water or N_2 inside the buncher.

4 Conclusions

In this paper, we have shown the results of an experiment aiming at cooling and bunching singly-charged light noble gas ions by means of a RFQCB installed on the beam line LIMBE at the GANIL facility. The following results have been obtained:

- Ions as light as $^4He^+$ have been cooled and bunched using H_2 as buffer gas. The total transmission through the device has been found of the order of 10 %.
- The "cooling" time, that is the time for the incoming ions to reach the bunching section of the device, has been found to be of the order of 300 μs for $^4He^+ + H_2$ and 800 μs for $^{40}Ar^+ + He$. Bunches of cooled $^4He^+$ ions have been produced with a time structure width of the order of 50 ns.
- Lifetime of the ions inside the buncher were measured by observing the fall-off of the transmission as a function of time up to a few tens of ms. A loss of ions in the case of $^4He^+$ has been observed due to charge transfer reactions. The value of the cross-section for charge transfer deduced from the evolution of the lifetime as a function of the buffer gas pressure is in agreement with previous measurements.
- Experimental data are in reasonnable agreement with the results of a microscopic Monte Carlo transport code.

The authors would like to thank warmly the technical staff members of LPC CAEN for help in the preparation of and during the experiment, in particular Ph. Desrues, Y. Merrer and C. Van Damme for the mechanical part of the experiment and J. Brégeault and Ph. Vallerand for the electronics.

Part of the set-up has been funded by the Region Basse-Normandie. This work was achieved and is pursued within the NIPNET Collaboration under contract HPRI-CT-2001-50034.

References

[1] P. van den Bergh, Nucl. Instrum. Meth. Phys. Res. B 126, 194 (1997)

[2] F. Herfurth, Nucl. Instrum. Meth. Phys. Res. A 469, 254 (2001)

[3] A. Nieminen, Nucl. Instrum. Meth. Phys. Res. A 469, 244 (2001)

[4] N. Maier, C. Boudreau, F. Buchinger, et al., Hyp. Int. 132, 521 (2001)

[5] G. Savard, R. C. Barber, C. Boudreau, et al., Hyp. Int. 132, 223 (2001)

[6] Y. Liu, J. F. Liang, G. D. Alton, et al., Rev. Sci. Instr. 73, 800 (2002)

[7] D. Rodriguez et al., in 3rd Conf. on Exotic Nuclei and Masses, edited by J. Aysto, Springer, Hmeenlinna, Finland,(2001)

[8] The SPIRAL Project, see the GANIL Web site: http://www.ganil.fr

[9] E. Liénard et al., Proceedings of the International Conference on Nuclear Physics at Border Lines, Lipari (Messina) Italy, editors G. Fazio, G. Giardina, F. Hanappe, G. Imme and N. Rowley, World Scientific, London, 2002, pp 176-179

[10] P. Herczeg, Prog. Part. Nucl. Phys. 46 (2001) 414

[11] P. Delahaye et al., Hyp. Int. 132, 479 (2001)

[12] G. Auger, F. Bocage, and B. Jacquot Technical Report GANIL R01-01, (2001)

[13] G. Auger and A. Peghaire, in Nouvelles du GANIL, Vol. 68 (2001)

[14] L. Maunoury, Thesis, University of Caen, 1998, (unpublished)

[15] L. Maunoury et al., Rev. Sci. Instr. 73, 561 (2002)

[16] D. A. Dahl, in 43rd ASMA Conference on Mass Spectrometry and Allied Topics, Atlanta, USA, (1995), p. 717

[17] G. Darius et al., to be published in Hyperfine Interactions

[18] G. Ban et al., *in preparation*

[19] G. Ban et al., *in preparation*

[20] H. W. Ellis et al., At. Data and Nuc. Data Tables 17, 177 (1976)

[21] H. W. Ellis et al., At. Data and Nuc. Data Tables 22, 180 (1978)

[22] H. W. Ellis, At. Data and Nuc. Data Tables 31, 113 (1984)

[23] L. A. Viehland and E. A. Mason, At. Data and Nuc. Data Tables 60, 37 (1995)

[24] H. Boehringer et al, J. Chem. Phys. 84, 1459 (1986)

Ion	Buffer Gas	T(%)
$^{4}He^{+}$	H_2	5-10
$^{22}Ne^{+}$	He,H_2	5-10
$^{40}Ar^{+}$	He	5-10
$^{40}Ar^{+}$	H_2	0

Table 1
Compilation of the transmissions obtained for the different pairs of ion-buffer gas constituents studied in this work.

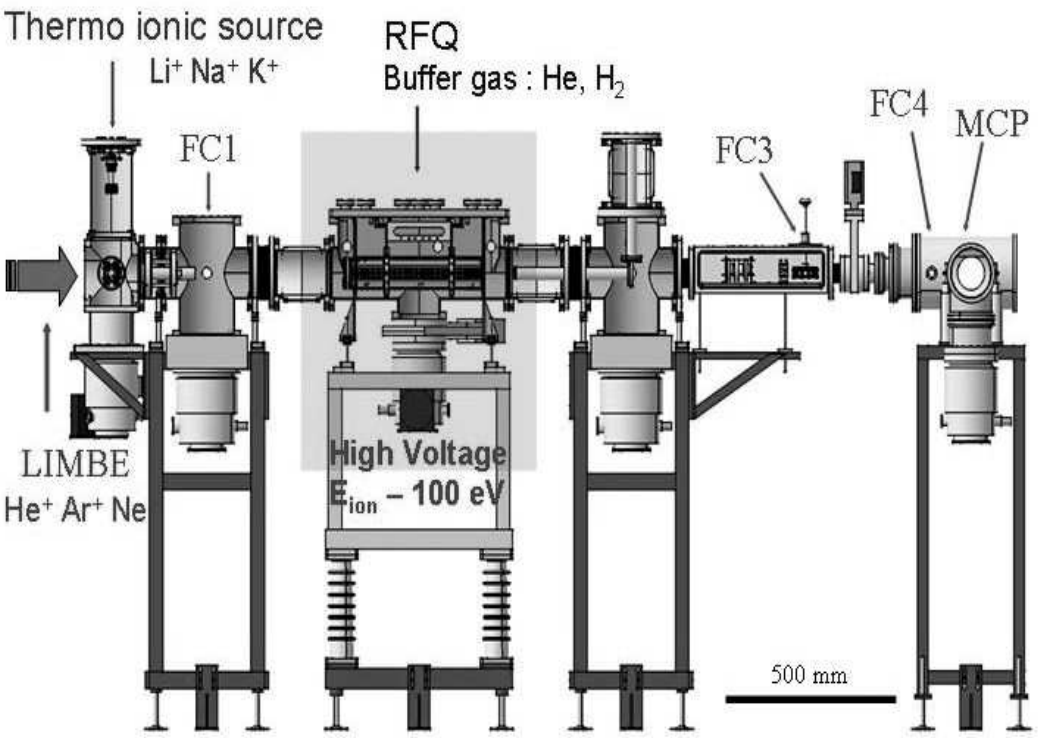

Fig. 1. *Schematic view of the experimental set-up.*

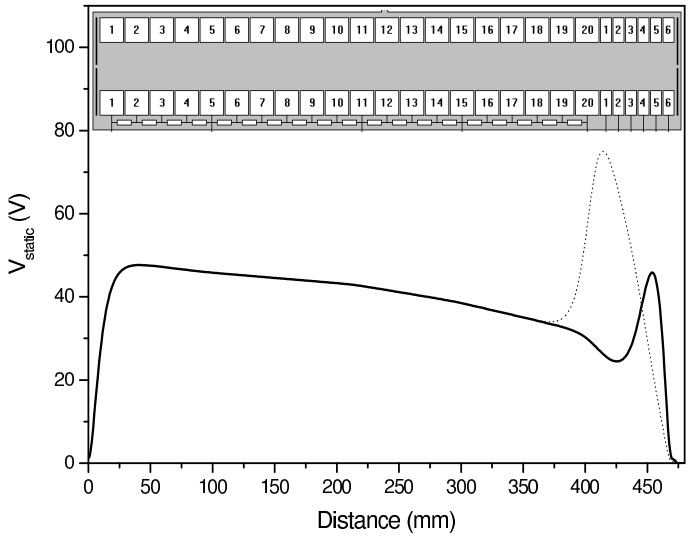

Fig. 2. *Electrostatic field along the symmetry axis as a function of the distance in the RFQCB for two different configurations. Configuration "storage" (thick line) allows to confine ions in a potential well inside the buncher while the configuration "extraction" (dotted line) pushes the ions outside the buncher. The last configuration is obtained by switching the voltage applied to the buncher electrodes. The geometry of the segmented electrodes constituting the cooler (labelled from 1 to 20 starting from the left) and the buncher (labelled from 1 to 6) is shown in the upper part of the figure. The values of the expected electric field with such a geometry have been obtained using the SIMION [16] software computer code. Potentials have been calculated with respect to the potential of the platform on which the device is placed.*

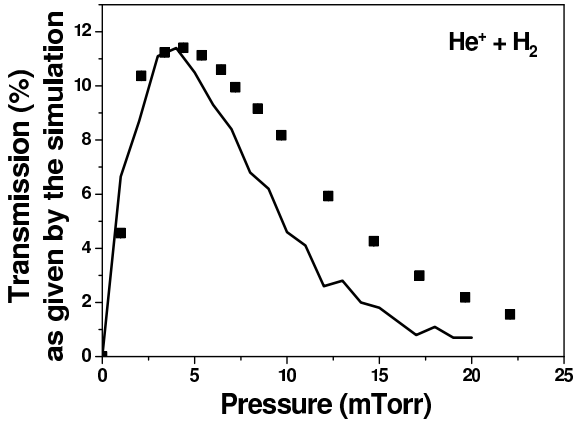

Fig. 3. *Transmission as a function of the pressure for $^4He^+$ ions extracted from the RFQCB using H_2 as buffer gas. Experimental data (black squares) have been normalized to the calculation (solid line) at the maximum value.*

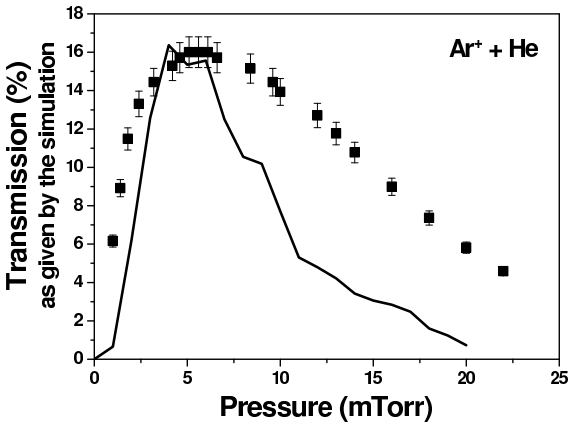

Fig. 4. *Same as Fig.3 but for* $^{40}Ar^{+}$ *ions and* He *as buffer gas.*

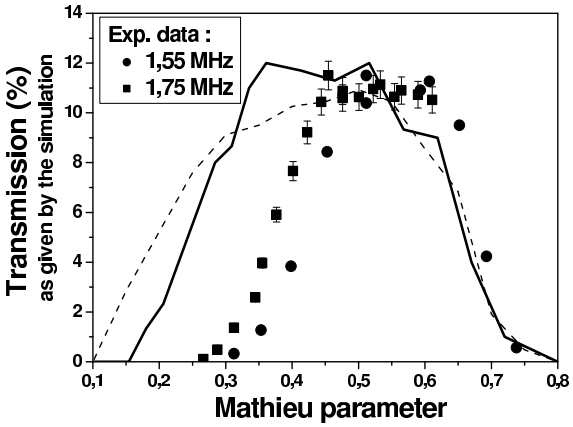

Fig. 5. *Transmission as a function of the Mathieu parameter for* $^{4}He^{+}$ *and* H_2 *as buffer gas. The two data sets correspond to two different values of the frequency* f*. For each fixed value of the frequency, the bias* V_0 *applied on the rods of the RFQCB was changed in order to scan the range of interest of the q parameter. Calculations: solid line (*f*=1.55 MHz), dashed line (*f*=1.75 MHz).*

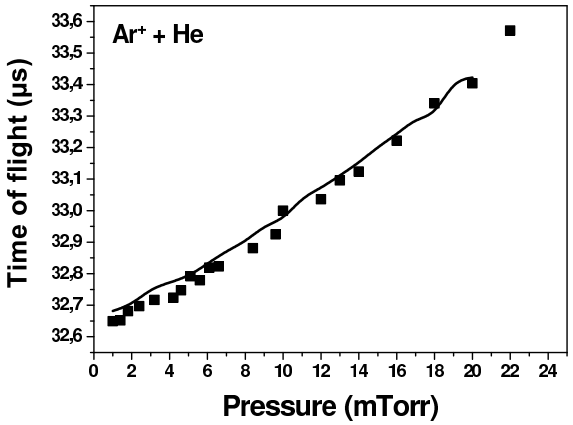

Fig. 6. *Mean time-of-flight distribution for $^{40}Ar^{+}$ ions after extraction from the RFQCB using He as buffer gas as a function of pressure. Black squares: experimental data, solid line: results of the simulation.*

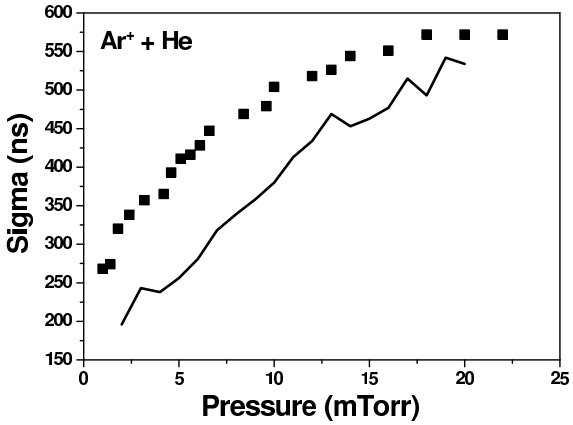

Fig. 7. *Width of the time-of-flight distribution under the same conditions than Fig.6.*

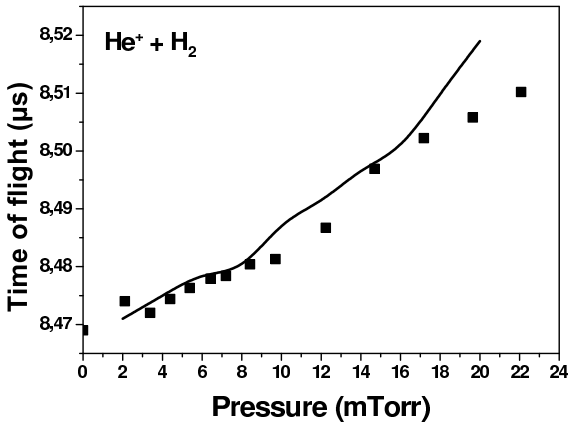

Fig. 8. *Same as Fig.6 but for $^{4}He^{+}$ ions and H_2 as buffer gas.*

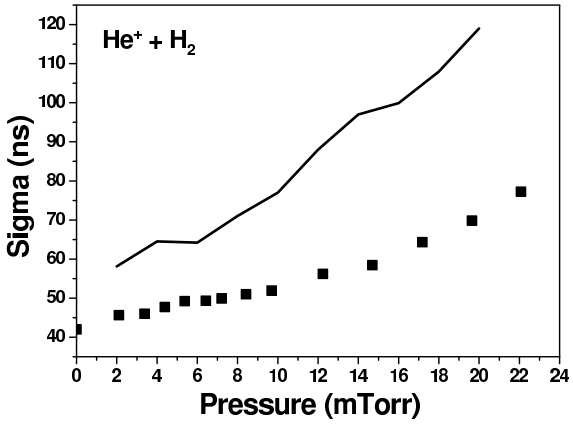

Fig. 9. *Same as Fig.7 but for $^4He^+$ ions and H_2 as buffer gas.*

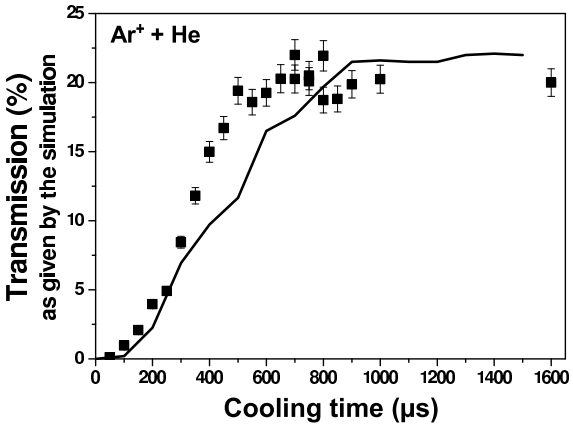

Fig. 10. *Transmission as a function of the 'cooling' time defined in the text. The ion is $^{40}Ar^+$ and the buffer gas is He. Black squares: experimental data, solid line: calculation.*

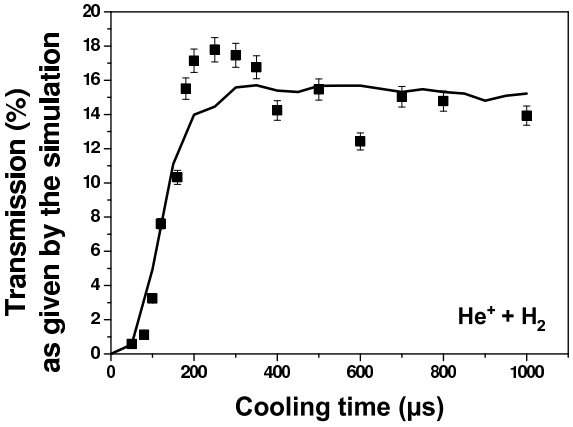

Fig. 11. *Same as Fig.10 but for $^4He^+$ ions and H_2 as buffer gas.*

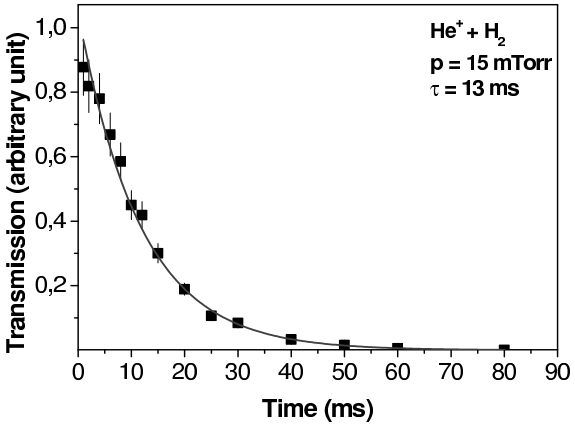

Fig. 12. *Lifetime measurement: transmission as a function of t_{cool} for $^4He^+$. The line corresponds to an exponential decay fit with a time constant of 13 ms. Here, the H_2 pressure is 15 mTorr.*

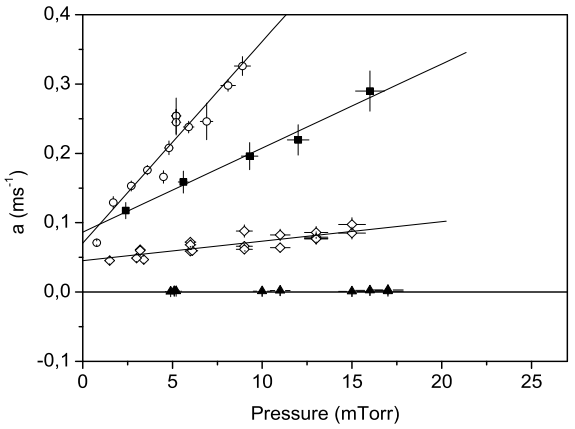

Fig. 13. *Evolution of $a = 1/\tau$ (in ms^{-1}) as a function of the pressure for various combinations of ion-buffer gas. Solid lines are the result of a linear fit according to Eq. 3. Black triangles: $Li^+ + H_2$, black squares: $^{22}Ne^+ + H_2$, open circles: $Li^+ + He$, open squares: $^4He^+ + H_2$.*